Volume : 4 | Issue : 2 | February 2015 • ISSN No 2277 - 8179

Research Paper

Study of the modeling and simulation of a membrane distillation unit coupled with solar collector

Engineering

KEYWORDS : solar collector; membrane distillation AGMD; mass transfer; Heat transfer; modeling.

Habib Ben Bacha	University King Saud University
Mokhless Boukhriss	LASEM (Laboratory Electro-Mechanical Systems), National Engineering School of Sfax,
Kmel Zarzoum	LASEM (Laboratory Electro-Mechanical Systems), National Engineering School of Sfax,
Khalifa Zhani	

ABSTRACT

Technology desalination of sea water in the presence of a membrane distillation unit driven by solar energy is a possible solution to reduce the energy costs of producing distilled water. In this work we will study the modeling and simulation of a solar system with a coupling unit membrane distillation. That latter port modeling and collector membrane distillation unit, into account the heat and mass transfer resistances associated with each element. The effects of adopting different functions, solar radiation conditions, configurations adopted in the system and the flow of membrane distillation module. Finally optimize a membrane distillation module for the higher water production.

1. Introduction

Membrane Distillation (MD) is a sorption process in which only the vapor molecules are transported across the hydrophobic microporous membranes. The driving force is the difference in vapor pressure between the feed side and the hot liquid to the cold filtrate side of the membrane. MD systems can be classified in four configurations depending upon the nature of the cold side of the membrane, the direct contact (DCMD), gap (AGMD), the sweep gas (SGMD) and empty (VMD). Several review articles have provided the fundamental principles of the MD [1-2]. Desalination is a significant demand for MD and configurations are commonly used DCMD and AGMD. In this study, the configuration is adopted for AGMD, wherein an air gap is interposed between the membrane and the condensing surface. Use of renewable energy for desalination offers a way to solve the problems of energy and water resources simultaneously. Different types of renewable energy can be adopted, such as solar thermal, solar photovoltaic, wind power, and geothermal energy as shown in the full document review by Kalogirou [3]. MD has the advantages of simplicity and the ability to operate with low-grade heat. MD solar desalination system driven, where energy is supplied entirely by flat plate solar thermal and photovoltaic panels, has been demonstrated by several research institutions [4-6] to be feasible and energetically competitive with other processes desalination.

The membrane distillation unit such AGMD conduit couples with the solar energy system of distillation desalination excluding photovoltaic devices, is shown in Fig.1.

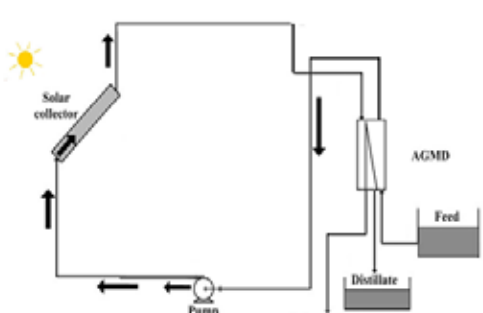

Figure.1: membrane distillation unit (AGMD) couples with solar collector

The main components are the solar collector and the MD module, but you can add a heat exchanger with a slack storage if we will work day and night. The MD module is featured with a design of energy [4, 5] recovery. System performance is determined by the profiles of solar radiation, the design of individual system components, component integration, the business model and the control strategy. Modeling and control methods of solar desalination, Ben Bacha et al. [7] and Roca et al. [8] presented studies for a solar cycle system condensation and evaporation multiple hybrid fossil fuel powered solar distillation system, respectively. Both groups have developed reduced process for integrating their control algorithms proposed on the basis of linear technology control and feedback linearization technique, models respectively.

Due to the intermittent and unpredictable nature of solar radiation, the steady state operation of the solar desalination process is not easy to achieve and the application of modern control algorithms is difficult.

The purpose of this study is to develop a dynamic model including models for key components, and the latter to investigate the overall system optimization. The model is built on platform [9], which allows the analysis and control system design.

2. Presentation of Methods for desalination

Figure 2 illustrates the desalination techniques classified into three broad categories: membrane processes, processes acting on the chemical bonds and processes being performed by phase change.

A method for separating salt water desalination in two parts: fresh water containing a low concentration of dissolved salts and concentrate brine. This process is energy-consuming. Various desalination techniques have been implemented over the years on the basis of the available energy [5].

Figure .2. Processes of desalination most used in the world

Volume : 4 | Issue : 2 | February 2015 • ISSN No 2277 - 8179

2.1. Basic principles of MD

MD was a membrane separation process combining with membrane technology and evaporation, and the membrane used was hydrophobic microporous membrane which could not be wetted by pending solutions. One side of membrane exposed to warm pending solutions directly (hot procedure side), the other side exposed to cold water solutions directly or indirectly (cold procedure side). Volatile components in hot procedure side evaporated in membrane surface, enter cold procedure side through membrane, and condensed into liquid phrase. Other components block off in hot procedure side by hydrophobic membrane and thus realize the objective of compounds separation and purification. MD was the process that transferred heat and quality simultaneously, and mass transfer impetus was steam differential imposed by components permeating through the both membrane sides.

2.2. Classification of MD

2.2.1. Direct contact membrane distillation (DCMD)

Both membrane sides contact with hot and cold water directly, respectively. It was suitable for water infiltration, such as desalination or condenses water solutions. DCMD has successfully been applied in the wastewater treatment, and resulted in some infiltrations with low pollution to environment, such as treating textile wastewaters, pharmacy wastewater containing taurine, water with heavy metal ions and so on. DCMD could be also used to separate heat-sensitive materials, such as the condensation of juice, blood and so on Chen and al [16]

2.2.2. Air gap membrane distillation (AGMD)

There was an air gap between cold procedure side and condensation wall, which could enhance the heat conduction drag. Therefore, flux of AGMD was usually smaller than that of other MDs, but AGMD had a broader application than DCMD, for AGMD condensed infiltration in the condensation surface, not directly. AGMD has been successfully applied in the production of pure water and the concentration of all kinds of nonvolatile solutes.

2.2.3. Sweep gas membrane distillation (SGMD)

Cold procedure side of membrane swept air in order to carry away the transferred steam. It used membrane to separate air or steam, in combination with lower heat conduction loss and lower mass transfer resistance. Infiltration condensed in the outer condenser. The charge of condenser was quite large, for in the large quantity of sweeping gas, only less vaporized filtration existed. Therefore, studies on SGMD were less available.

2.2.4. Vacuum membrane distillation (VMD)

Steam was continuously exerted from the cold procedure side of membrane by vacuum system, and condensed outside of the membrane separator. Porous membrane used in VMD served as the support of gas-liquid surface. This membrane possessed some selectivity, based on Knudsen diffusion rate of diffusing substances, but separation extent was mainly determined by the gas-liquid equilibrium condition in the membrane-solution surface. Compared to other MDs, one of the advantages was that heat conduction loss by membrane could be neglected. As a new separation approach, it was mainly applied to eliminate the volatile components in dilute aqueous solutions (Liu and al [17] with larger membrane flux and greater industrial practical significance.

3. Modeling of system components

Studied the flow stream is represented as shown in Fig. 1. The fluid flow, absorbing the thermal energy of the solar collector is supplied completely in a distillation unit of the air gap spiral (AGMD) Module [4, 5] is designed with a function of recovery energy, the cold sea water is first introduced into the cold side of the heat exchange module with hot water, then further heated in the solar collector sea, and return to the hot side of the module. 1-D models for individual components are formulated and solved numerically on the platform, where the membrane module can be developed via a graphical interface and model components are linked and solved in a system based on the equations so. Component specifications analyzed in this study are references in Table 1 with the list of [4, 5, 10, 11].

3.1. Solar collector

The solar collector retained in this study is the most common flat collector (FPC). CEP-coated with a pipe or conduit for transporting the heat transfer fluid, or an acrylic glass panel covered absorber plate on top, and the insulation on the sides and bottom. A schematic illustration of the manifold is shown in Fig. 3.

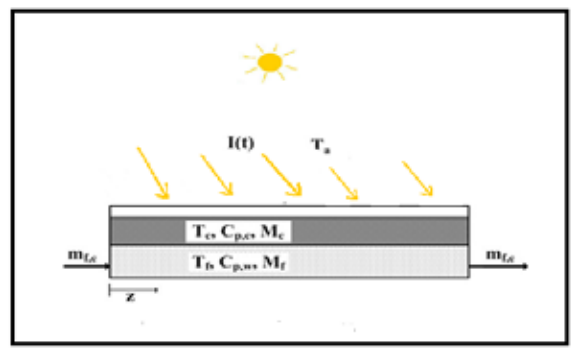

Figure.3: model of flat plate solar collector

Equations of energy balance for the absorber and the fluid are given in the equations. (1) and (2), as shown:

$$\frac{dTc}{dt} = \frac{SU'}{Mc\,C_{p,c}}\left(\frac{BI(t)}{U'} + T_a(t) - T_c\right) - \frac{Sh_c}{Mc\,C_{p,c}}(Tc - Tf) \quad (1)$$

$$\frac{\partial T_f}{\partial t} = -L_c\frac{m_{f,c}}{M_f}\frac{\partial T_f}{\partial z} + \frac{Sh_c}{Mf\,C_{p,w}}(Tc - Tf) \quad (2)$$

For the fluid, in addition to taking into account the assumption of a single 1-D temperature change, the temperature is below 100 ° C, so no evaporation occurs. For that the collector is well insulated, the loss on the sides or bottom heat is neglected.

3.2. Membrane distillation unit

The system uses AGMD modules. For Module with size specifications listed in Table 1, the unfolded screen is shown in Fig. 4.

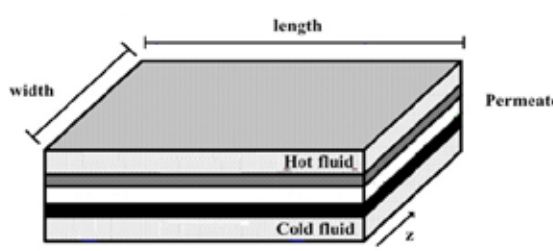

Figure.4: AGMD model

The hot fluid and hot fluid is against the current. For simplicity, seawater is used, along with hot and cold fluids in the model. For the purpose of this study is to investigate the optimization and control of the entire system, this simplification will not cause significant differences in the test results. The mass transfer resistance of the hot fluid side is insignificant in a previous analysis [12] to the hollow fiber module. Transferring the mass flow is determined by taking into account the mass transfer resistance in the gap and membrane. However, the heat transfer

resistance of the whole layers is taken into account. Mass and energy flows for all layers, including the hot fluid, the membrane gap, a cold fluid and metal sheet are illustrated by Fig. 5 and 6 and the model equations are summarized below.

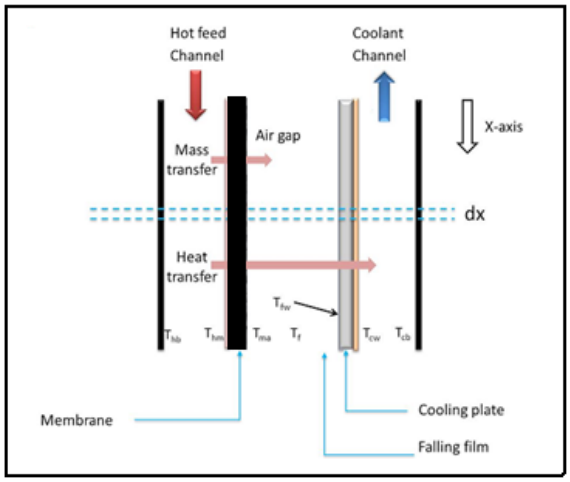

Figure.5: AGMD model for heat transfer and mass

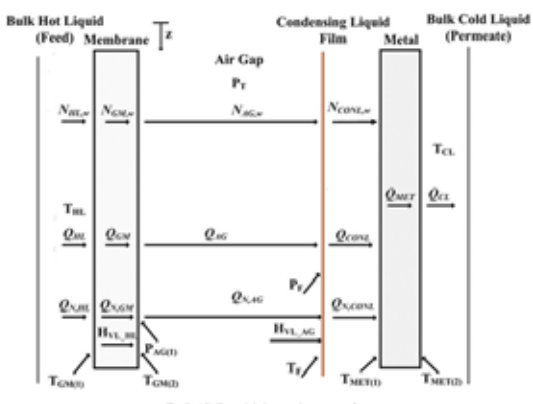

Figure.6: the model parameters AGMD for heat transfer and mass

The mass balances

$$\frac{dm_{f,HL}}{dz} = -N_{GM,W} L_W M_W \quad (3)$$

$$\frac{dm_{f,CONL}}{dz} = -N_{AG,W} L_{MD} M_W \quad (4)$$

$$N_{GM,W} = N_{AG,W} \quad (5)$$

Balancing the energy

$$\frac{\partial T_{HL}}{\partial t} = -W_{MD}\left[\frac{m_{f,HL}}{M_{HL}}\frac{\partial T_{HL}}{\partial z} + \frac{L_{MD}}{M_{HL} C_{p,HL}}\left(h_{HL} + N_{GM,W} C^{L}_{p,W} M_W\right)\left(T_{GM(1)} - T_{GM(2)}\right)\right] \quad (6)$$

$$\frac{\partial T_{CL}}{\partial t} = -W_{MD}\left[\frac{m_{f,CL}}{M_{CL}}\frac{\partial T_{CL}}{\partial z} + \frac{L_{MD} h_{CL}}{M_{CL} C_{p,CL}}\left(T_{MET(2)} - T_{CL}\right)\right] \quad (7)$$

$$Q_{HL} + Q_{N,HL} - H_{VL,HL} = Q_{GM} + Q_{N,GM} \quad (8)$$

$$Q_{GM} + Q_{N,GM} = Q_{AG} + Q_{N,AG} \quad (9)$$

$$Q_{AG} + Q_{N,AG} + H_{VL,AG} = Q_{CONL} + Q_{N,CONL} \quad (10)$$

$$Q_{MET} = Q_{CONL} + Q_{N,CONL} \quad (11)$$

$$Q_{MET} = Q_{CL} \quad (12)$$

Mass fluxes

$$N_{GM,W} = \frac{k_{GM,W}}{RT_{GM,arg}}\left(P^{sat}_{GM(1),W} - P^{sat}_{AG(1),W}\right) \quad (13)$$

$$N_{AG,W} = \frac{k_{GM,W}}{RT_{arg} P_{tm,air}\ \delta_{AC}}\left(P^{sat}_{AG(1),W} - P^{sat}_{F,W}\right) \quad (14)$$

Heat fluxes

$$Q_{HL} = h_{HL}(T_{HL} - T_{GM(1)}) \quad (15)$$

$$Q_{GM} = [\varepsilon h_{GM} + (1+\varepsilon) h_{MEM}](T_{GM(1)} - T_{GM(2)}) \quad (16)$$

$$Q_{AG} + Q_{N,AG} = h_{AG\frac{\theta}{\varepsilon-\theta}}\left(T_{GM(2)} - T_F\right) \quad \text{Avec} \quad \theta = NCp/h \quad (17)$$

$$Q_{CONLL} = h_{CONL}(T_F - T_{MET(1)}) \quad (18)$$

$$Q_{MET} = h_{MET}(T_{MET(1)} - T_{MET(2)}) \quad (19)$$

$$Q_{CL} = h_{CL}(T_{MET(2)} - T_{CL}) \quad (20)$$

$$Q_{N,HL} = N_{GM,N} C^{L}_{p,W}\left(T_{HL} - T_{GM(1)}\right) \quad (21)$$

$$Q_{N,GM} = N_{GM,N} C^{L}_{p,W}(T_{GM(1)} - T_{GM(2)}) \quad (22)$$

$$Q_{N,CONL} = N_{AG,W} C^{L}_{p,W}(T_F - T_{MET(1)}) \quad (23)$$

$$H_{VL,HL} = H_{GM,W} \Delta H_{vap,W} \quad (24)$$

$$H_{VL,AG} = H_{AG,W} \Delta H_{vap,W} \quad (25)$$

The heat transfer coefficients for hot and cold fluid sides are estimated using the correlations reported by Schock and Miquel [15] for the module spiral wound membrane.

$$\mathrm{Nu} = 0.065.\,\mathrm{Re}^{0.875}.\,\mathrm{Pr}^{0.25} \quad (26)$$

For the condensing heat transfer to the film, the following relationship is employed: [13]

$$h_{CONL} = 0.943\left[\frac{\rho^{L}_{W}\left(\rho^{L}_{W} - \rho^{V}_{W}\right) g\, \Delta H_{vap,W} k^{L}_{W}}{L_{MD}\, \mu_W\, (T_{CONL} - T_{MET})}\right] \quad (27)$$

With the model, the optimization study is channeled to two different solar radiation profiles, as shown in Fig. 7

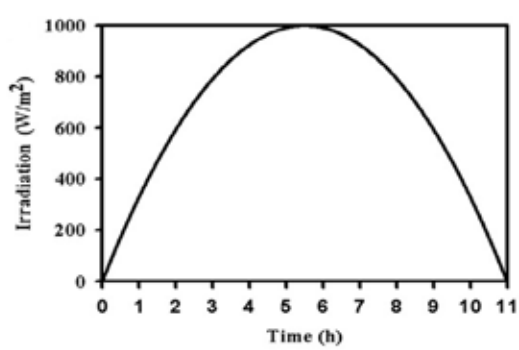

Figure.7: solar irradiation profiles

Volume : 4 | Issue : 2 | February 2015 • ISSN No 2277 - 8179

4. Results of simulation of distillation unit components

4.1. Simulation for membrane distillation unit

For the porous membrane, the mass transfer and heat transfer analysis reflect molecular diffusion and the Knudsen and steam and conduction membrane material respectively.

Regarding the gap, the molecular diffusion and thermal conduction are considered the results of the simulation model are found AGMD varying production rate with the feed fluid and the flow temperature [4.14] as shown in Fig. 8(a et b) .

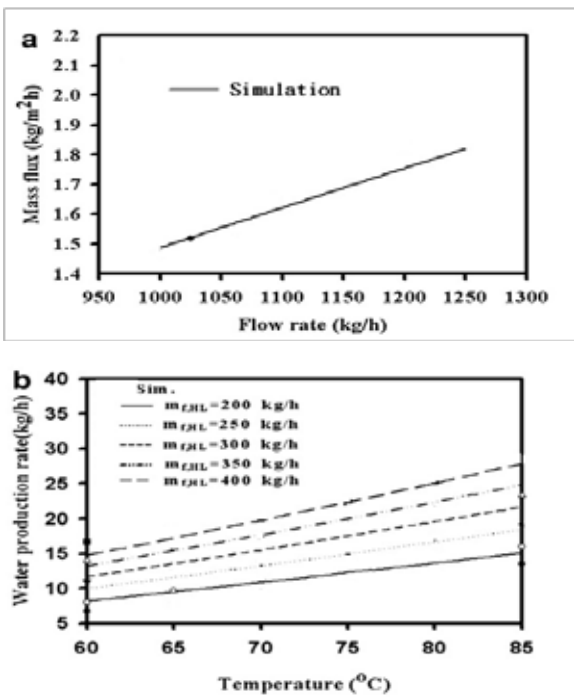

Fig. 8.the resultant of simulation data from (a) [5] and (b) [19]

Using AGMD model, effects of heat and mass of the membrane and the air gap are studied by varying the heat transfer coefficients and mass simultaneously by a factor of 0.1 or 10. The results are shown in Fig. 9.

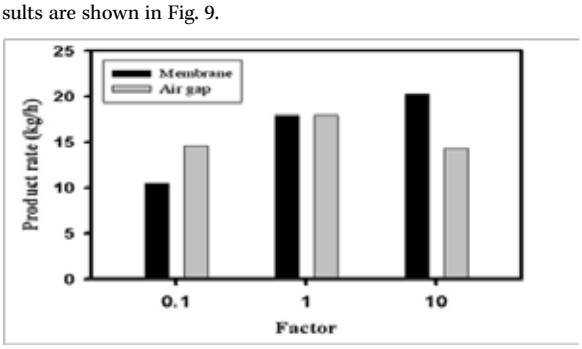

Fig. 9. Effects of heat and mass transfers on water flux.

For the membrane, increase transfer coefficients results in improved production rates and the effect is more important in decreasing direction. However, the air gap, the production rate decreases in the two directions of the change transfer coefficients. The reason is that the increased heat transfer coefficient result in lower operating temperature and hence the reduction in the rate of pipe production.

4.2. Simulation of solar water

A steady state simulation of the solar collector water was used to study the influence of the variation of the water inlet temperature, fluid flow, solar flux and the ambient temperature on the outlet temperature of water.

• Effect of the water flow

Figure 10 illustrates the variation of the water temperature at the sensor output (fs) depending on the different values of the water flow (mf) for the following operating conditions: Tamb = 15 ° C, Tfe = 20° C, I = 800W / m².

Figure 10 shows that the water temperature at the sensor output decreases by increasing the flow rate of the water flowing through the solar collector water. From this figure, it can be drawn after a flow of water of about 0.08 kg / s, the decrease in the outlet temperature is lower, and a flow rate of about 0.12 kg / s, the curve became rather insensitive to increase water flow.

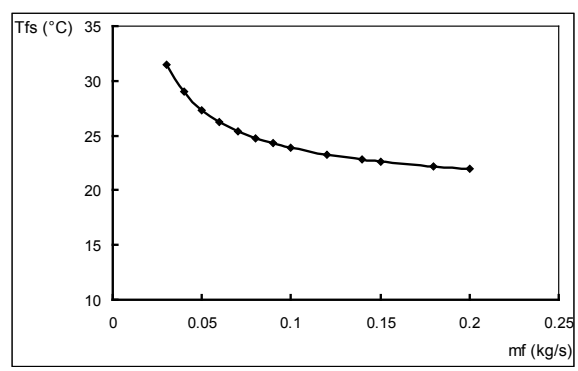

Figure .10. Changing the outlet temperature as a function of water flow

• Effect of sunlight on the flow rate and the temperature difference of the output and input water sensor

In this part of the attention has focused initially on the variation of the outlet temperature of the fluid as a function fs fluid flow and sunlight. However, the fluid temperature (Tfe) to the sensor input is not always constant since it depends on the temperature of the external environment (Tamb). So to compare different rates for Tfs must study the variation of the gap (fs - fe). Ie, it must seek the temperature increase that can provide the collector for each flow.

Figure 11, we can conclude that the size (fs - fe) for a constant flow rate increases for an increase in solar flux. At low water flow rates (for example 0.01 kg / s) and for the same value of solar intensity, the difference between the outlet temperature of the fluid and that of the input is higher than that for relatively high flow rates (e.g. 0.2 k / s).

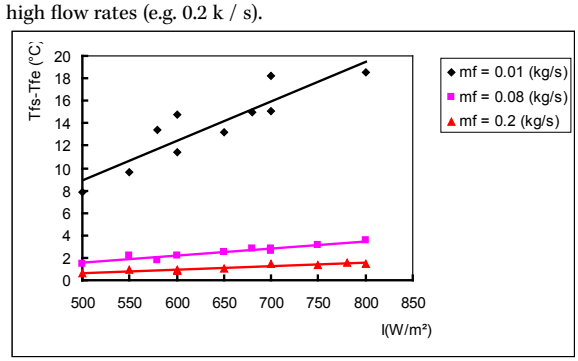

Figure .11. Gap outlet temperatures and sensor input depending on the flow I and

5. The design distillation unit and solar collector

Based on the above findings, a complete design of the integrated solar energy system has been developed and briefly presented above.

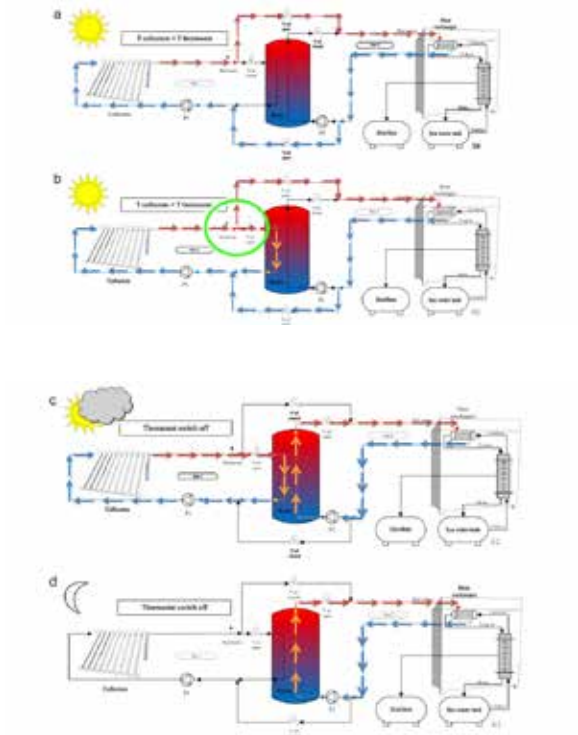

Figure .11. The design distillation unit

The distillation unit design torque solar has 4 different configurations, as shown in the diagrams below (Fig. 12 a - d). It should be noted that, for reasons of clarity, in these heat exchanger systems and the MD unit are shown separately, but is integrated in the driver design system. In addition, in order to allow continuous operation of the system, make-up system of a power or high coolant supply is also provided, but not shown in the drawings. Based on the above design, a system is built will be placed soon and will be tested the technical feasibility and performance evaluation in the coming months.

6. Conclusions

The conduit of membrane distillation unit of the spiral wound gap for solar desalination system has been studied by the dynamic model development for all components. A numerical study was conducted to study the behavior of this unit by varying the main parameters farms, namely the feed rate, heat supply inlet temperature of the air gap configuration (the channel the air gap is designed and constructed to allow its use as a standard air gap, impregnate evacuated gap and gap). With a variation of the water flow distillate, with higher values s for the higher feed flow rate and temperature. The thermal energy consumption was extremely high, due to the very significant heat recovery in the laboratory scale unit MD.

A simplified model of the system was also developed, implemented in a spreadsheet. The model is based on heat and mass conservation equations of works taken from previous literature and completely without adjustable parameters, allowing its use as a predictive tool. Model was used to perform a simplified analysis of process performance and economic analysis of the MD unit e modeling predictions for the unity of MD, the study suggests optimizing the use of the single tank configuration higher production rates. In addition, the objective function which takes into account both the rate of production and the thermal energy absorption provides better performance results. A design of a solar prototype was performed leading to full identification of design parameters and operating regimes. This unit will be built and tested in 2015....

Table n °1: lists of membrane parameters and solar collector

AGMD module		solar collector	
Membrane area (m^2)	10	Absorber surface area (m^2)	6
Width (m)	1.29	Effective absorptivity	0.8
Length (m)	0.7	Heat transfer coefficient of loss to atmosphere (W/m^2K)	4
Thickness (mm)	0.14	Heat transfer coefficient between absorber and fluid (W/m^2K)	458
Pore diameter (mm)	0.2	Mass of absorber (kg)	250
Porosity	0.77	Heat capacity of absorber (J/kg K)	460
Tortuosity	1.9		
Thermal conductivity (W/m K)	0.173		
Hot liquid channel thickness (mm)	0.77		
Cold liquid channel thickness (mm)	0.77		
Air gap channel thickness (mm)	0.43		
Metal foil thickness (mm)	0.98		
Thermal conductivity (W/m K)	398		

Volume : 4 | Issue : 2 | February 2015 • ISSN No 2277 - 8179

Nomenclature

A area ($m^{2)}$
B effective absorptivity
Cp heat capacity (J/kg K)
D diffusion coefficient (m2/s)
Fj objective functionj

H height (m)
HVL heat transfer rate of phase change (J/m2s)
h heat transfer coefficient (W/m2K)
I intensity of solar radiation (W/m2)
K thermal conductivity (W/m K)
Kc proportional gain
Ku ultimate gain
k mass transfer coefficient (m/s)
L length (m)
M mass (kg)
Mw molecular weight of water (kg/kmol)
mf fluid flowrate (kg/s)
N Mass flux (kmol/m2s)
OP controller output
P pressure (Pa)
Q heat transfer rate (J/s)
QN sensible heat transfer rate (J/s)
R gas constant (J/kmol K)
S collector absorber surface area (m2)
Si stream number i
T temperature (K)
U overall heat transfer coefficient of the heat exchanger (W/m2K)
U' overall heat loss coefficient between the collector absorber and the surroundings (W/m2K)
W width (m)
DHvap heat of vaporization (J/kmol)
D thickness (m)
e membrane porosity
m viscosity (kg/m s)
r density (kg/m3)
s membrane tortuosity
sI integral time (s)
su ultimate period (s)
L liquid
G gas
Sat saturated
AG air gap
A Ambient
Air air
Avg average
c solar collector
CL cold liquid
CONL condensate liquid
F condensing film surface in the air gap
F circulation fluid in the solar collector
fh circulation fluid between the coil and the heat exchanger
fs circulation fluid between the internal coil and the solar collector
GM gas in the membrane
HL hot liquid
MD membrane module
MEM membrane
MET metal
Nu Nusselt number
Pr Prandtl number
Re Reynolds number
T total
w water
wa watereair

REFERENCE

[1] Lloyd DR, Lawson KW. Membrane distillation. Journal of Membrane Science 1997;124:1-25. | [2] Bourawi MS, Ding Z, Ma R, Khayet M. A framework for better understanding membrane distillation separation process. Journal of Membrane Science 2006;285:4-29. | [3] Kalogirou SA. Seawater desalination using renewable energy sources. Progress in Energy and Combustion Science 2005;31:242-81. | [4] Banat F, Jwaied N, Rommel M, Koschikowski J, Wieghaus M. Performance evaluation of the "large SMADES" autonomous desalination solar-driven membrane distillation plant in Aqaba, Jordan. Desalination 2007;217:17-28. | [5] Banat F, Jwaied N, Rommel M, Koschikowski J, Wieghaus M. Desalination by a"compact SMADES"autonomous solar-powered membrane distillation unit.Desalination 2007;217:29-37. | [6] van Medevoort J, Jansen A, Hanemaaijer JH, Dotremont C, Nelemnas B, van Sonsbeek E, et al. Memstill: seawater desalination a solution to water scarcity.In: BMG-NMG membrane Symposium. Antwerp, Belgium; November 16,2008. | [7] Ben Bacha H, Bouzguenda M, Damak T, Abid MS, Maalej AY. A study of a water desalination station using the SMCEC technique: production optimization. Renewable Energy 2000;21:523-36. | [8] Roca L, Berenguel M, Yebra L, Alarcón DC. Preliminary modeling and control studies in AQUASOL project. Desalination 2008;222:466-73. | [9] Aspen Technology, Inc. Aspen custom modeler. Version. Cambridge, Massachusetts, USA: Aspen Technology, Inc; 2006. | [10] Ben Bacha H, Damak T, Bouzguenda M, Maalej AY, Ben Dhia H. A methodology to design and predict operation of a solar collector for a solar-powered desalination unit using the SMCEC principle. Desalination 2003;156:305-13. | [11] Avlonitis S, Hanbury WT, Ben Boudinar M. Spiral wound modules performance an analytical solution: part II. Desalination 1993;89:227-46. | [12] Chang H, Liau JS, Ho CD, Wang WH. Simulation of membrane distillation modules for desalination by developing user's model on Aspen Plus platform. Paper accepted for publication by Desalination. | [13] Holman JP. Heat transfer. McGraw-Hill; 1989. | [14] Koshchikowski J, Wieghaus M, Rommel M. Solar thermal-driven desalination plants based on membrane distillation. Desalination 2003;156:295-304. | [15] Schock G, Miquel A. Mass transfer and pressure loss in spiral wound modules.Desalination 1987;64:339-52. | [16] Chen, C.X., Yu, L.X., & Dai, T.Y. (1996). Review of new membrane and membrane process. Technology of Water Treatment, 22(6):307-313. | [17] Liu, L.Y., Ding, C.W., & Chang, L.J., et al. (2008). Progress in membrane separation enhanced by ultrasound. Chemical Industry and Engineering Progess,27(4):32-37. |